

# Thermal-hydraulic Design and CFD Analysis of Fuel Assembly for China Lead-based Research Reactor

Tao ZHOU\*, Zengfang GE, Shuyong LIU, Yunqing BAI, Yong SONG

Key Laboratory of Neutronics and Radiation Safety, Institute of Nuclear Energy Safety Technology, Chinese Academy of Sciences, Hefei, Anhui, 230031, China

tao.zhou@fds.org.cn

## Abstract

Chinese Academy of Sciences had launched a Strategic Priority Research Program to develop Accelerator Driven System (ADS) for nuclear waste transmutation since 2011. China Lead-based Research Reactor (CLEAR-I) was selected as the reference reactor system in China ADS project. In this contribution, the hottest fuel assembly (FA) in the core was selected as the analysis object; 3D CFD analysis of the hottest FA thermal-hydraulic was carried out. The results show that: 1) the key parameters including Liquid Lead-Bismuth (LBE) mass flow rate, cladding temperature are lower than the corresponding design limits; 2) wires play an important role in mixing the coolant to make stronger turbulence intensify in center sub-channels of FA than edge and corner sub-channels; 3) the friction factor decreases in the entrance region of FA then fluctuates periodically in the fully developed region, while the steep decline of Nusselt number has taken place in the entrance of active zone, and then decrease smoothly to zero near the outlet of active zone.

**Keywords:** China Lead-based Research Reactor (CLEAR-I), Thermal-hydraulic, Fuel assembly

## 1. INTRODUCTION

The accelerator driven system (ADS) is the most promising system in terms of the partitioning and transmutation strategies for the radioactive waste in the advanced nuclear fuel cycle. The Strategic Priority Research Program named “Advanced Nuclear Fission Energy-ADS Transmutation System” has been launched by Chinese Academy of Sciences since 2011 [1]. Institute of Nuclear Energy Safety Technology, Chinese Academy of Sciences who carried out a lot of work in the design and technologies of heavy liquid metal cooled reactors during recent years, including low activation materials [2-8], liquid metal [9-10], sub-critical system [11-12], and advanced nuclear software [13-16] were taking charge of the reactor system in China ADS project. China LEAad-based research Reactor (CLEAR-I) was selected as reference reactor for ADS system in the first stage of China ADS project, liquid lead-bismuth (Pb-Bi) eutectic were used as the primary coolant, four main heat exchangers and two pumps laid out in the main vessel to transfer thermal power to the secondary coolant by the forced circulation of the primary cooling system.

In this work, based on the conceptual design of CLEAR-I, thermal-hydraulic design of fuel assembly (FA) for CLEAR-I was described and preliminary 3D detail thermal-hydraulic of FA was carried out using CFD tools. The analysis results can be able to support the optimize design of FA.

## 2. DESIGN DESCRIPTION

## 2.1 Primary Cooling System Description

CLEAR-I aimed to build a flexibility test platform for different operation modes and different nuclear fuels testing, so CLEAR-I had critical and subcritical dual-mode operation. According to the experimental object and implementation procedure, the deeply sub-criticality and low power mode will be operated on the first step, and then the power will increase by adding FAs or increasing proton intensity step by step. In this paper, critical operation mode of CLEAR-I was selected as analysis scenario.

CLEAR-I reactor thermal power is  $10\text{MW}_{\text{th}}$ , and it is cooled by LBE driven by mechanical pump in the primary cooling system. The pressurized liquid water is adopted as the secondary coolant, and the air cooler is the ultimate heat sink. Fig.1 shows the structural design of CLEAR-I reactor.

As shown in Fig.1, in the primary cooling system two main pumps and four shell and tube heat exchangers are uniformly located in the liquid LBE pool of main vessel, called as the integrated pool structure. There is a hot barrier and an insulation layer in the central position of the LBE pool dividing the LBE pool into internal and external parts. The  $300^{\circ}\text{C}$  LBE flows upwards and heated by the FAs, then collected in the hot LBE pool in the upper of the core. The average temperature of the mixed LBE reaches  $380^{\circ}\text{C}$ . After passing through the upper inlet window of the heat exchanger, the hot LBE enters into the shell side of the heat exchanger where the hot LBE is cooled by secondary liquid water in the tube side. Then the LBE flows out from the lower outlet window of the heat exchanger to the cold LBE pool, finishing the circulation of the primary cooling system.



Fig.1 Overview of reactor system

## 2.3 FA design

In CLEAR-I core, the FA has the 61-pins wires fixed structure, and total length of pin is 1675mm. The structure of fuel pin is composed of the several parts: upper and lower end caps, tighten spring, upper and lower reflectors, active zone, gas chamber and ballast. Fuel pins are arranged in a triangular pitch, main geometry parameters are listed in Table.1.

Table.1 FA and pin geometry parameters of CLEAR-I

Parameter	Value
Total fuel pin length (mm)	1675
Active height (mm)	800
Pin pitch (mm)	13.68
Pin cladding thickness (mm)	0.4

Pin outer diameter (mm)	12
Wire diameter (mm)	1.5
FA pitch (mm)	375
Number of pins per FA	61

### 3. SIMULATION MODEL DESCRIPTION

#### 3.1 Mathematical model

In the simulation, the liquid LBE physical properties change with temperature. Main properties of liquid LBE calculated are as follow [17]:

- 1) **Density, Kg/m<sup>3</sup>**

$$\rho = 11096 - 1.3236 \times T_{coolant}$$

- 2) **Heat capacity at constant pressure, J/(Kg·K)**

$$C = 159.0 - 2.72 \times 10^{-2} \times T_{coolant} + 7.12 \times 10^{-6} \times T_{coolant}^2$$

- 3) **Thermal conductivity, W/(m·K)**

$$\lambda_{coolant} = 3.61 + 0.01517 \times T_{coolant} - 1.741 \times 10^{-6} \times T_{coolant}^2$$

- 4) **Dynamic viscosity, Pa·s**

$$\eta_{coolant} = 4.94 \times 10^{-4} \times \exp\left(\frac{754.1}{T_{coolant}}\right)$$

In order to understand the regular of cross-stream velocity in axial section, the non-dimensional cross-stream velocity is adopted in this paper and defined as:

$$(U_x^2 + U_y^2)^{1/2} / U_z$$

The friction factor is defined as [18]

$$f = \frac{-(dp/dz)D_h}{\rho U_{in}^2/2}$$

Based on the average cladding surface temperature of all the pins and the global bulk lead-bismuth temperature, the global Nusselt number at any axial position is defined as [18]:

$$Nu = \frac{q(D_h/\lambda_{coolant})}{[1/N \cdot \sum_{i=1}^N (T_S)_i - T_{coolant}]}$$

Where:

$D_h$  is hydraulic diameter of the bundle (=4×flow area/wetted perimeter)

N is total number of pins in the bundle

P is the pressure of coolant

q is the heat flux

$T_{coolant}$  is the coolant temperature at any axial section

$T_S$  is the average cladding temperature at any axial section

$\lambda_{coolant}$  is the coolant thermal conductivity

$U_{in}$  is the inlet velocity

$U_x$ 、 $U_y$ 、 $U_z$  is the velocity component in x、y、z.

$\rho$  is the coolant density

$z$  is the axial distance

### 3.2 MODEL AND BOUNDARY CONDITIONS

#### 3.2.1 Geometric model and simulation mesh

As shown in Fig 2, the FA is chosen as the simulation model, which includes active zone, counter weight, upper & lower gas chamber and upper & lower reflector. The length of zone under active zone is 670mm, while 140mm for the zone length above active zone. The model between fuel pin and wire is simplified from line contact to face contact easy to mesh generate.

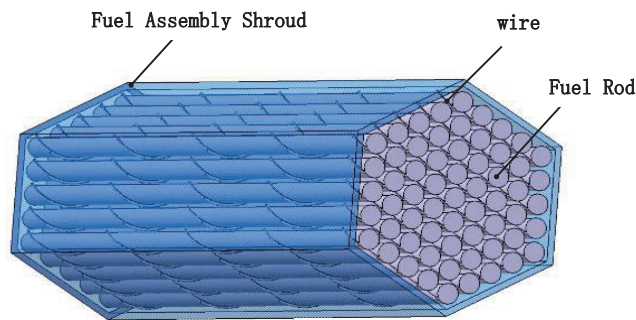


Fig.2. Simulation model of FA

In this work, ICEM has been adopted for generate hexahedral mesh, and the total block number is more than 0.5 million. Grid independency has been tested by varying the grids in cross-stream direction and varying the axial grids. The finished mesh distribution is shown in Fig 3. There are 112 meshes around the circumference of fuel pin, 404 for axial meshes, and 37.03 million for total meshes. Using these meshes, the value of  $y^+$  is lower than 15, so it better meets the simulation requirements.

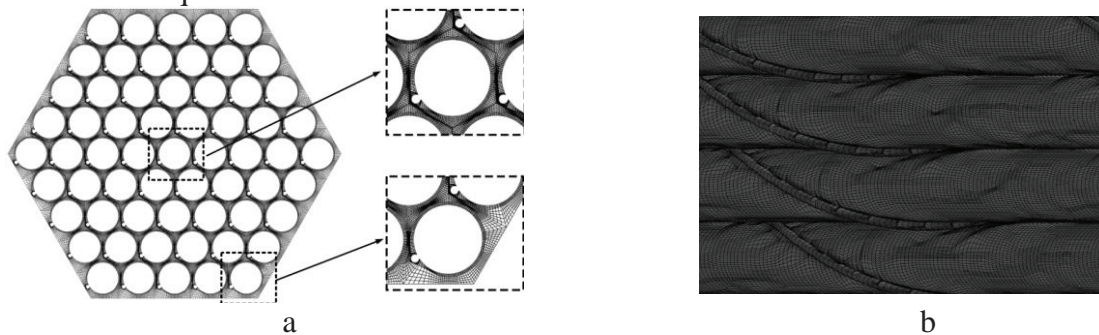


Fig.3 Computational grids distribution of helical wire-wrapped FA

#### 3.2.2 Simulation model

The CFD simulations were performed by the general business software ANSYS 14.0 CFX, and SST(Shear Stress Transport) k- $\omega$  model was adopted for the simulations, because SST k- $\omega$  model was proved to be suitable for simulate the thermal-hydraulic phenomenon of wire wrapped FA in the liquid heavy metal environment[19-20].

The SST  $k-\omega$  model is selected for the boundary layer, and the  $k-\epsilon$  model for the core region. So there is a mixing phenomenon between each other.

In the CFX simulation model turbulence numeric is high resolution, advection scheme is high resolution, and heat transfer model is thermal energy.

### 3.2.3 Boundary conditions

In this paper the hottest FA is chosen as reference. To reflect the actual thermal hydraulic phenomenon for CLEAR-I FA, the boundary conditions of model is as follow. The non-slip wall boundary condition was applied for all the surfaces of fuel pins and wires. A constant mass flow rate and pressure are selected as inlet and outlet boundary conditions respectively, as shown in Table.2. Based on the power distribution of the fuel pins calculated by core physics as shown in the Fig 4, heat flux is chosen as the pin wall boundary condition in the active zone. However the power distribution along the axial direction of fuel pins follows the law of approximate cosine distribution. The mass flow rate of the hottest FA is obtained by thermal-hydraulic design at the CLEAR-I conceptual design stage, and the simulation results are relatively conservative.

**Table.2 Boundary conditions for CFX simulation**

Parameter	Value
Inlet mass flow rate (Kg/s)	13.9
Inlet temperature (K)	573
Outlet pressure (Pa)	0

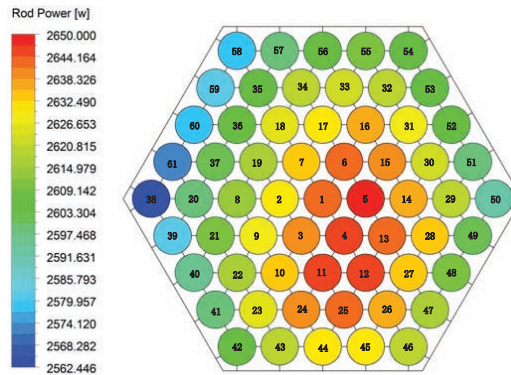


**Fig. 4 The power distribution of the fuel pins**

## 4. RESULTS

### 4.1 Flow pattern

The path lines of the wire-wrapped tube bundles are shown in Fig.5. The path line along the flow direction presents the regular of cyclic and symmetric natures. The flow is more complicated in wire-wrapped FA, particularly along the wire winding direction. The continued changes in the direction of wire wrapped could induce the large cross flow mixing because of a contribution for the radial and tangential velocity components.

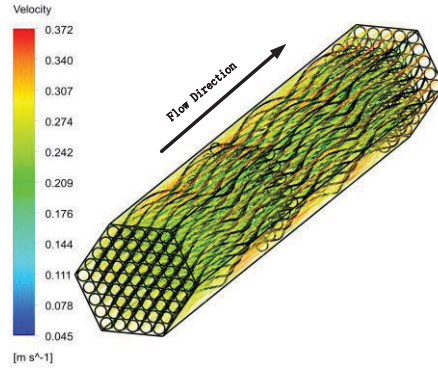


**Fig.5 Flow path lines**

The outlet velocity distribution is shown in Fig.6. The right figure of the Fig.6 details the enlarged scale of center, edge and corner sub-channels velocity and tangential section vector. Due to higher flow resistance offered by the tubes and wire, the velocity in the center sub-channels is less than other sub-channels. The velocity values in the edge and corner sub-channels are nearly the same. The sweeping flow region generally offers lower flow resistance than the mixing flow region, so there is more uniform velocity in the mixing zone than the sweeping regime. The sweeping flow in the edge and corner sub-channels (near the hexagonal wall) is predominant in the FA upstream zone.

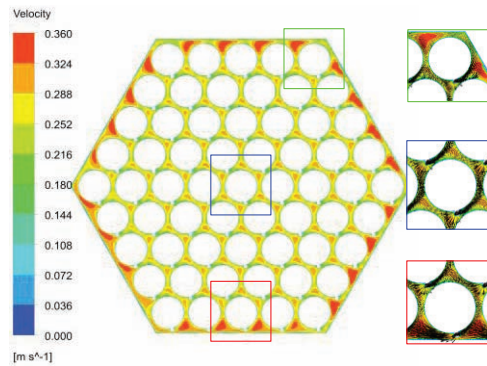


**Fig.6 Velocity distribution at outlet**

The non-dimensional cross-stream velocity along axial direction presents in Fig.7. There is a steep increase for cross-stream velocity which is fully developed nearly at  $L/D_h \approx 40$ . In the fully developed region, the cross-stream velocity oscillates periodically along the axial distance near a mean value with the small finite amplitude. In the active zone, the coolant is heated, which impact the cross-stream velocity distribution in cross section. Due to the outlet effects, there is a small reduction nearly at outlet.

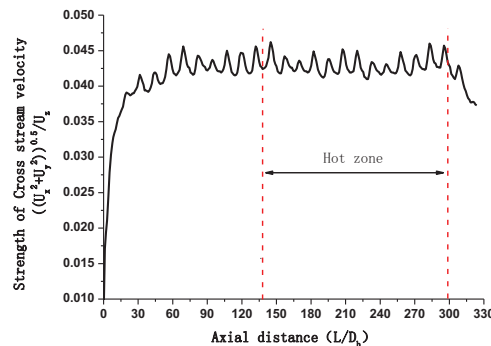


**Fig.7 Non-dimensional cross-stream velocity**

## 4.2 Temperature distribution of the flow domain

The contours of temperature in flow direction section are shown in Fig.8. Before the coolant enters the active zone, the temperature keeps in the constant value, and then gradually increases along the flow direction of active zone. The regular of the temperature distribution in active zone section keep the same law described as follows.

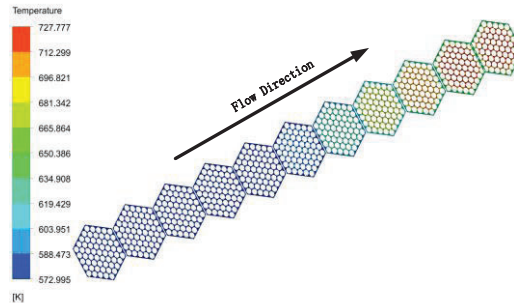


**Fig.8** Temperature contours in the flow direction section

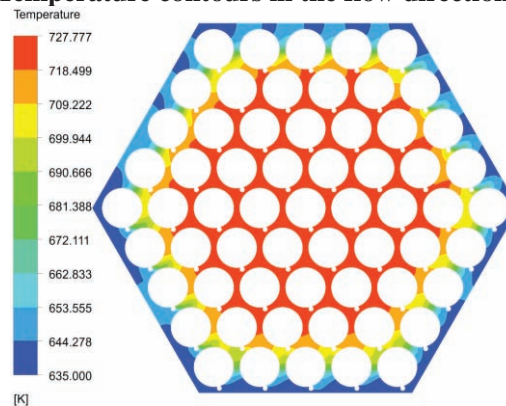


**Fig.9** Temperature distributions outlet

The cross-stream flow is responsible for promoting good mixing and hence a nearly uniform temperature as shown in Fig.9. It is clearly seen from the figure that the temperature values are higher in the center sub-channels compared to edge and corner sub-channels. The follow reasons may contribute to the temperature distribution: firstly, all surrounding tubes contribute to the rise of temperature in the center zone, whereas the walls do not contribute to rise in temperature for the edge/corner sub-channels; secondly, the sweeping flow patterns in the center sub-channels and mixing flow patterns in the edge/corner sub-channels, which contribute to significant difference in heat transfer; thirdly, the power distribution of the fuel pins in the center sub-channels is higher than others as shown in Fig.4.

## 4.3 Fuel cladding temperature distribution

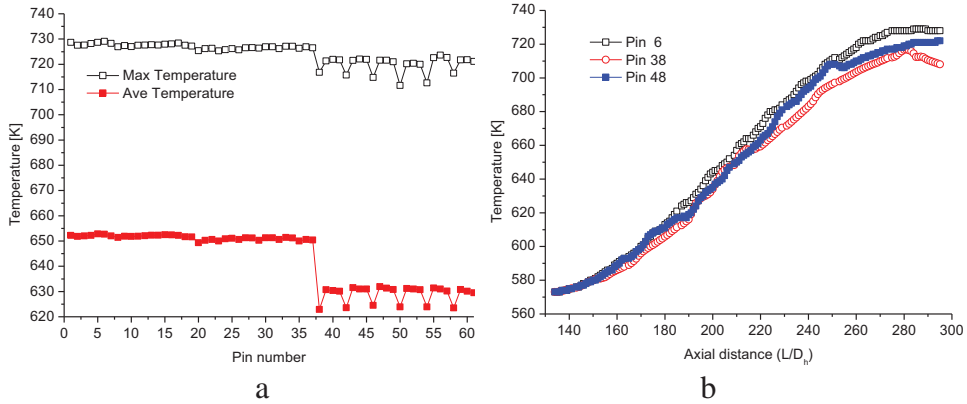


**Fig.10 Temperature in the fuel cladding surface**

Fig.10 shows the fuel cladding surface maximum and average temperature, the maximum and average temperature of the pin number from 1 to 37 in the similar axial distance are higher than others. The pin (fuel pin number is 38, 42, 46, 50, 54, 58) in the edge sub-channels have the lowest cladding temperature. This phenomenon due to the fuel power distribution is shown in Fig.4 and the flow patterns described in section 4.1 and 4.2.

The fuel cladding temperature of typical fuel pin is depicted in Fig.10 b. The cladding temperature rapidly increases along the active zone, and then tends to a constant value or decreases. The maximum temperature occurs near the active zone outlet, and the cladding temperature is 729K in the pin 6, which is lower than the design safety criteria of fuel cladding temperature 823K.

#### 4.4 Friction factor and Nusselt number development

The friction factor variation curve along axial direction is present in Fig.11 a. There is a steep decline in friction factor in the entrance region of FA, then it attains full development nearly at  $L/D_h \approx 40$ . In the fully developed region, the friction factor oscillates periodically along the axial distance near a mean value with the small finite amplitude.

The development of Nusselt number along the axial direction is shown in Fig.11 b. A steep decrease occurs in the entrance of active zone, and then Nusselt number decreases smoothly, which tends to zero for the low heat flux near the outlet of active zone.

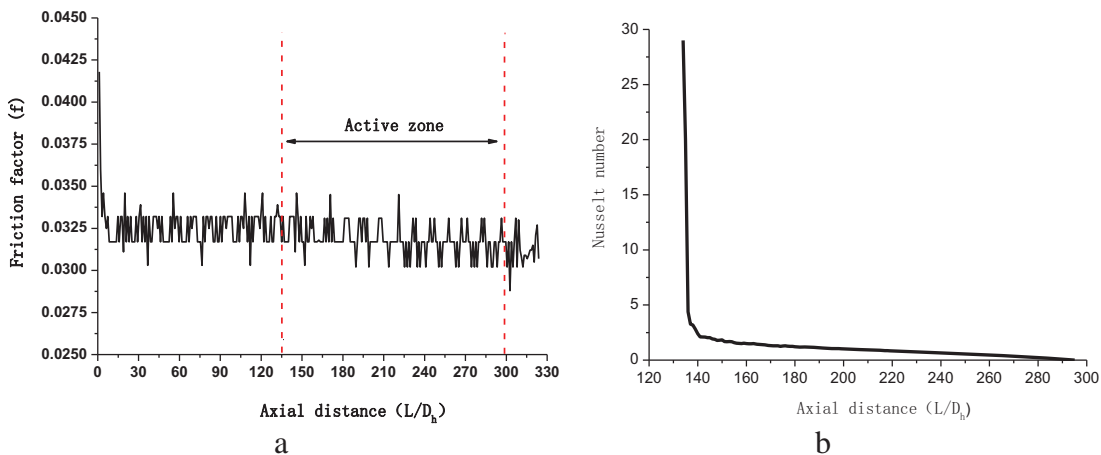


**Fig.11 Friction factor and Nusselt number development along axial direction**

## 5. CONCLUSIONS

This contribution gives the thermal-hydraulic parameter design for the hottest FA of CLEAR-I and using CFD tools to analyze 3-D thermal-hydraulic characteristics. The difference power distribution for all pins and along the axial direction was considered as the boundary in this simulation. Flow patterns and temperature distributions in the whole FA was simulated. Major findings of the present work are as follows:

- 1) In the CFD simulation, it is necessary to take the reality power distribution as the boundary for the FA, and only in this way the calculation results are believable.
- 2) The velocity in the center sub-channels is less than other sub-channels due to higher resistance offered by the tubes and wire. The velocity values in the corner and edge sub-channels are almost the same.
- 3) The flow is fully developed at  $L/D_h \approx 40$  before entering the active zone, the mean value of the friction factor and non-dimensional cross-stream velocity in the fully development region oscillate periodically along the axial distance near a mean value with small but finite amplitude. Nusselt number decreases smoothly in the whole active zone.
- 4) Wires play an important role in mixing the coolant to make stronger turbulence intensify in center sub-channels of FA than edge and corner sub-channels. And it leads to the uniform temperature distribution in center sub-channels.
- 5) The maximum cladding temperature occurs near the FA outlet but below the corresponding design constraints.

These results show the preliminary thermal-hydraulic design of the hottest FA for CLEAR-I is feasible and can be able to support the optimize design of CLEAR-I FA. In the next work, the flow blockage of FA will be analyzed to study the transient safety characteristics of CLEAR-I FA.

## ACKNOWLEDGMENTS

This work was supported by “Strategic Priority Research Program” of Chinese Academy of Sciences (No.XDA03040000), National Natural Science Foundation of China (No. 91026004) and Natural Science Foundation of China under grant No.51076166. We further thank the great help from other members of FDS Team in this research.

## REFERENCES

- [1] Zhan Wenlong, Xu Hushan. Advanced Fission Energy Program: ADS Transmutation System[J]. Bulletin of Chinese Academy of Sciences, 2012, 27(3):375-381(in Chinese)
- [2] Q.Y. Huang, N. Baluc, Y. Dai, et al. Recent Progress of R&D Activities on Reduced Activation Ferritic/Martensitic Steels[J]. Journal of Nuclear Materials, 2013, 442(1-3): S2-S8
- [3] Q.Y. Huang, S. Gao, Z.Q. Zhu, et al. Progress in Compatibility Experiments on Lithium-Lead with Candidate Structural Materials for Fusion in China[J]. Fusion Engineering and Design, 2009, 84:242-246
- [4] Q.Y. Huang, J. Li, Y. Chen. Study of Irradiation Effects in China Low Activation Martensitic Steel CLAM. Journal of Nuclear Materials, 2004, 329:268-272
- [5] Q.Y. Huang, Y.C. Wu, J. Li, et al. Status and Strategy of Fusion Materials Development in China. Journal of Nuclear Materials, 2009, 386-388:400-404
- [6] L. Qiu, Y. Wu, B. Xiao, et al. A Low Aspect Ratio Tokamak Transmutation System. Nuclear Fusion, 2004, 40:629-633.
- [7] Q.Y. Huang, C. Li, Y. Li, et al. Progress in Development of China Low Activation Martensitic Steel for Fusion Application. Journal of Nuclear Materials, 2007, 367-370:142-146.
- [8] Y.C. Wu, Q.Y. Huang, Z. Zhu, et al. R&D of Dragon Series Lithium Lead Loops for Material and Blanket Technology Testing. Fusion Science and Technology. 2012, 62-1:272-275.
- [9] Y.C. Wu, the FDS Team. Design Status and Development Strategy of China Liquid Lithium-Lead Blankets and Related Material Technology[J]. Journal of Nuclear Materials, 2007, 367-370:1410-1415
- [10] Y.C. Wu, FDS Team. Design Analysis of the China Dual-functional Lithium Lead (DFLL) Test Blanket Module in ITER[J].

Fusion Engineering and Design, 2007, 82: 1893-1903

- [11] Y.C. Wu, Y.Q. Bai, Y. Song, et al. Study on the conceptual design for china lead-bismuth research reactor[J]. Nuclear Science and Engineering, 2014,34: 201-208 (Chinese)
- [12] Y.C. Wu, J.Q. Jiang, M.H. Wang, et al. A Fusion-Driven Subcritical System Concept Based on Viable Technologies[J]. Nuclear Fusion, 2011, 51(10):103036
- [13] Y.C. Wu, G. Song, R.F. Cao, et al. Development of Accurate/Advanced Radiotherapy Treatment Planning and Quality Assurance System (ARTS)[J]. Chinese Physics C (HEP & NP), 2008, 32(Suppl. II):177-182
- [14] Y.C. Wu, J. Song, H. Zheng, et al , CAD-Based Monte Carlo Program for Integrated Simulation of Nuclear System SuperMC[J]. Annals of Nuclear Energy, DOI: 10.1016/j.ANUCENE.2014.08.058.
- [15] Y.C. Wu, FDS Team. CAD-Based Interface Programs for Fusion Neutron Transport Simulation. Fusion Engineering and Design, 2009,84(7-11), 1987-1992.
- [16] Y.C. Wu, Z. Xie, U. Fischer. A Discrete Ordinates Nodal Method for One-Dimensional Neutron Transport Calculation in Curvilinear Geometries. Nuclear Science and Engineering, 1999, 133(3): 350-357.
- [17] Handbook on Lead-bismuth Eutectic Alloy and Lead Properties, Materials Compatibility, Thermal-hydraulics and Technologies. 2007
- [18] N. Govindha, K. Velusamy, T. Sundararajan, et al. Simultaneous development of flow and temperature fields in wire-wrapped fuel pin bundles of sodium cooled fast reactor[J]. Nuclear Engineering and Design, 267 (2014) 44-60
- [19] F. R. Menter, Two-equation eddy-viscosity turbulence models for engineering applications, AIAA J, 32, pp.269-289, 1994.
- [20] Xu Cheng, Nam-il Tak. Investigation on turbulent heat transfer to lead-bismuth eutectic flows in circular tubes for nuclear applications. Nuclear Engineering and Design 236 (2006) 385-393